EUROPHYSICS LETTERS 1 March 1999

Europhys. Lett., **45** (5), pp. 638-644 (1999)

Reactions at polymer interfaces: Transitions from chemical to diffusion-control and mixed order kinetics

B. O'Shaughnessy[1] and D. Vavylonis[2]

[1] *Department of Chemical Engineering, Columbia University*
500 West 120th St., New York, NY 10027, USA
[2] *Department of Physics, Columbia University*
538 West 120th St., New York, NY 10027, USA

(received 24 April 1998; accepted in final form 21 December 1998)

PACS. 82.35+t – Polymer reactions and polymerization.
PACS. 05.40−a – Fluctuation phenomena, random processes, noise, and Brownian motion.
PACS. 68.10−m– Fluid surfaces and fluid-fluid interfaces.

Abstract. – We study reactions between end-functionalized chains at a polymer-polymer interface. For small chemical reactivities (the typical case) the number of diblocks formed, $\mathcal{R}_t$, obeys 2nd-order chemically controlled kinetics, $\mathcal{R}_t \sim t$, until interfacial saturation. For high reactivities (*e.g.*, radicals) a transition occurs at short times to 2nd-order diffusion-controlled kinetics, with $\mathcal{R}_t \sim t/\ln t$ for unentangled chains while $t/\ln t$ and $t^{1/2}$ regimes occur for entangled chains. Long-time kinetics are 1st order and controlled by diffusion of the more dilute species to the interface: $\mathcal{R}_t \sim t^{1/4}$ for unentangled cases, while $\mathcal{R}_t \sim t^{1/4}$ and $t^{1/8}$ regimes arise for entangled systems. The final 1st-order regime is governed by center-of-gravity diffusion, $\mathcal{R}_t \sim t^{1/2}$.

In many technological applications, interfaces in polymeric multicomponent materials are reinforced through chemical bonding [1]. Techniques of reinforcing interfaces separating immiscible polymer species involve attaching functional groups to a certain fraction of the bulk chains [2, 3]. Under melt conditions, reactions produce copolymers (see fig. 1) which serve as interfacial bridges, enhancing interfacial fracture toughness and yield stress after cooling [4]. In commercial applications ("reactive processing") the two melts are simultaneously mechanically mixed. In addition to their direct reinforcing effect, the copolymer products also help to produce a finer blend morphology by reducing interfacial tension and preventing the coalescence of minority phase droplets during mixing [2].

Due to the importance of such applications, recent theoretical and numerical research efforts have focused on understanding the reaction kinetics at polymer-polymer interfaces at a fundamental level [5-8], in the simplest case of end-functionalized chains (see fig. 1). These studies have addressed only a small fraction of the available parameter space. They emphasized the limit of "infinitely" reactive groups, *i.e.* local chemical reactivities Q of order $1/t_a$ where t_a is the monomer relaxation time. In fact, such Q values are realized only for exotic

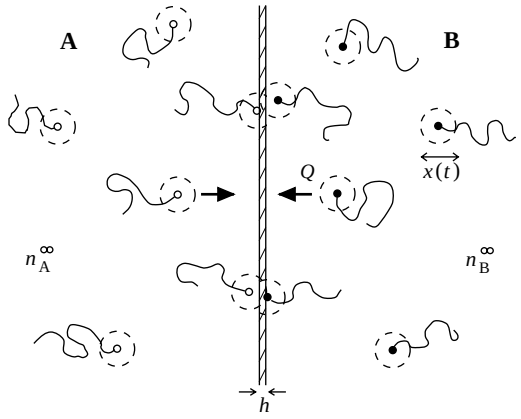

Fig. 1. – End-functionalized chains reacting at an interface separating immiscible melts A, B containing functional groups, of local reactivity Q, whose initial densities are n_A^∞, n_B^∞. For short times, reactions are confined to those groups whose exploration volumes of size $x(t)$ overlap at the interface. The number of such pairs per unit area is $x^4(t) n_A^\infty n_B^\infty$.

species such as radicals (or electronically excited groups as in model photophysical systems) whilst chemical reactivities employed in most reactive blending experiments are extremely small. A typical example is the reaction between carboxylic acid and epoxide ring groups for which $Qt_a \approx 10^{-11}$ [9]. In addition, with the exception of ref. [7], previous studies have been confined to reactive chains very dilute in an unreactive melt background.

In this letter we develop a theory for the kinetics of reactions between end-functionalized chains at a stationary interface separating immiscible melts A and B (see fig. 1). Our approach is quite general in terms of chemical reactivity, molecular weight, and number densities of reactive ends in each bulk, n_A^∞ and n_B^∞. The convention throughout is that A reactants are more dilute, $n_A^\infty \leq n_B^\infty$. We will construct "phase diagrams", representing various classes of reaction kinetics, in the density-reactivity plane for both unentangled and entangled polymer melts.

The principal conclusions of this study are as follows: 1) For the usual case of small reactivities, $Qt_a \lesssim 10^{-6}$, the behavior is as follows. Chemically controlled 2nd-order kinetics apply at short times, with number of reactions per unit area, $\mathcal{R}_t$, increasing as $\mathcal{R}_t \sim t\, n_A^\infty n_B^\infty$. If $n_A^\infty \approx n_B^\infty$, these kinetics persist until crowding of the interface by A-B diblocks strongly suppresses further reactions. However, for n_A^∞ sufficiently smaller than n_B^∞, then before the interface gets saturated a crossover occurs to 1st-order diffusion-controlled (DC) kinetics with $\mathcal{R}_t \approx x(t)\, n_A^\infty$, where $x(t)$ is the rms monomer displacement in time t. 2) For the case of highly reactive groups, $Qt_a \approx 1$, irrespective of density a crossover occurs from 2nd- to 1st-order kinetics at long times. In addition, a new 2nd-order DC regime appears during which $\mathcal{R}_t \approx x^4(t)\, n_A^\infty n_B^\infty$.

Our aim is the reaction rate, $\frac{\mathrm{d}}{\mathrm{d}t}\mathcal{R}_t$. To begin, we observe that this requires calculation of the 2-body correlation function ρ_{AB}^s, proportional to the number of A-B reactive groups in contact at the interface: $\frac{\mathrm{d}}{\mathrm{d}t}\mathcal{R}_t = Qha^3\rho_{AB}^s(t)$. Here h is the width of the interface and a the monomer size. Unfortunately, the exact dynamical equation for ρ_{AB}^s involves 3-body correlations. It is in fact impossible to write a closed exact equation for ρ_{AB}^s, since correlation functions of all orders are coupled in an infinite hierarchy of dynamical equations. This complication which arises in all many-body reacting systems is typically resolved by approximating 3-body correlations in terms of lower-order correlation functions [10]. However, in ref. [11] (where a general theory for

interfacial reaction kinetics was developed) after postulating much less restrictive bounds on the magnitude of 3-body correlation functions, we obtained the following closed self-consistent equation for $\rho^s_{\rm AB}$:

$$\rho^s_{\rm AB}(t) \approx n^\infty_{\rm A} n^\infty_{\rm B} - \lambda \int_0^t {\rm d}t'\, S^{(4)}_{t-t'}\, \rho^s_{\rm AB}(t') - \lambda n^\infty_{\rm B} \int_0^t {\rm d}t'\, S^{(1)}_{t-t'}\, \rho^s_{\rm AB}(t') \quad \lambda \equiv Qha^3\,, \qquad (1)$$

where $S^{(4)}_t \approx 1/x^4(t)$ is the probability density [5] that in the absence of reactions an A-B pair is in contact at the interface at t, given its members were in contact at the interface initially. $S^{(1)}_t \approx 1/x(t)$ is the probability density an A or B group, initially at the interface, returns to it after time t. (Equation (1) is closed in terms of the degrees of freedom describing the reactive end-groups only. To achieve this, it has implicitly been assumed that reactions do not modify equilibrium internal polymer chain configurations [12]. There is considerable evidence from renormalization group analyses [13] that this approximation correctly captures all scaling dependencies, though prefactors are unreliable.) Equation (1) is a closed system in terms of $\rho^s_{\rm AB}$; though spatial degrees of freedom in the bulk have been integrated out, the behavior of $\rho^s_{\rm AB}$ reflects bulk correlation functions. For example, the signature in eq. (1) of a reaction-induced density "hole" near the interface is domination of the $n^\infty_{\rm A} n^\infty_{\rm B}$ and $S^{(1)}$ terms (these 2 terms then balance one another). On the other hand, a depletion hole in the bulk *2-body* correlation function corresponds to a balance of the $n^\infty_{\rm A} n^\infty_{\rm B}$ and $S^{(4)}$ terms [11]. In the following, instead of directly solving eq. (1) for $\rho^s_{\rm AB}$, we will rather motivate the solutions using physical arguments. The reader may then verify the results by direct substitution into eq. (1).

Consider the reaction rate at short times. Initially, reactive groups are distributed as in equilibrium, $\rho^s_{\rm AB} \approx n^\infty_{\rm A} n^\infty_{\rm B}$. Hence initial kinetics are 2nd order, $\mathcal{R}_t \approx \lambda t\, n^\infty_{\rm A} n^\infty_{\rm B}$. However, reactions may perturb equilibrium correlations. Consider times shorter than t_l, the diffusion time corresponding to a distance of order the typical separation between the more dense B reactive groups, $x(t_l) = (n^\infty_{\rm B})^{-1/3}$. For $t < t_l$ reactions are due to the few isolated A-B pairs which happened to be initially within diffusive range, *i.e.* within $x(t)$ of one another near the interface (see fig. 1). After time t, the number of times such a pair has collided, $\mathcal{N}_{\rm coll}$, is of order the number of encounters the A makes with the interface, $(t/t_a)(h/x(t))$, multiplied by the probability it meets the B, $a^3/x^3(t)$, during each of these encounters. Hence the total reaction probability, $Qt_a\mathcal{N}_{\rm coll} \approx \lambda t/x^4(t)$ is increasing with time provided the dynamical exponent z characterizing monomer diffusive dynamics, $x(t) \sim t^{1/z}$, is greater than or equal to 4 (the case $z = 4$ is marginal, but it can be shown to be similar to $z > 4$). Now for times shorter than τ, where τ is the longest polymer relaxation time, values of z are either 4 or 8 [14]. This implies that the pair reaction probability is increasing with time and hence there exists a timescale t^*_2, obeying $x^4(t^*_2)/t^*_2 = \lambda$, after which all such A-B pairs will have reacted. Thus for $t > t^*_2$ non-equilibrium correlations develop ($\rho^s_{\rm AB}$ is no longer equal to $n^\infty_{\rm A} n^\infty_{\rm B}$) and a depletion hole grows in the 2-body correlation function. $\mathcal{R}_t$ is then proportional to the number of pairs per unit area which diffusion could have brought together by time t, $\mathcal{R}_t \approx x^4(t) n^\infty_{\rm A} n^\infty_{\rm B}$. These are 2nd-order diffusion-controlled kinetics.

For how long do these DC kinetics persist? For $t > t_l$, since at least one B lies within the exploration volume of any A within $x(t)$ of the interface, thus any such A must have reacted. For $t > t_l$, a depletion hole thus grows in the A density field and the reaction rate becomes controlled by the diffusion of A species to the interface, $\mathcal{R}_t \approx x(t) n^\infty_{\rm A}$. These are 1st-order DC kinetics. In summary,

$$\mathcal{R}_t \;\approx\; \lambda\, t\, n^\infty_{\rm A} n^\infty_{\rm B} \;\xrightarrow{t^*_2}\; x^4(t)\, n^\infty_{\rm A} n^\infty_{\rm B} \;\xrightarrow{t_l}\; x(t)\, n^\infty_{\rm A} \quad (t^*_2 < t_l < \tau,\;\; S^{\rm conc})\,. \qquad (2)$$

Notice that while the more dilute side controls the long-time reaction rate, it is the more

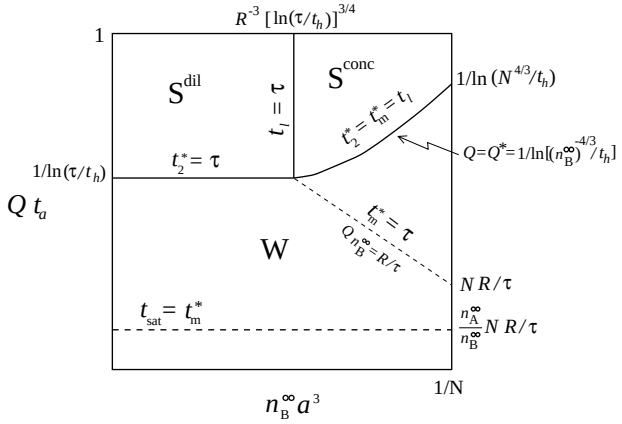

Fig. 2. – Unentangled melts, reaction kinetics "phase diagram" in Q-$n_{\rm B}^\infty$ plane. Axes are logarithmic and units chosen such that $t_a = a = 1$. Maximum possible density is $n_{\rm B}^\infty a^3 = 1/N$ (all chains functionalized). Kinetics are qualitatively distinct in the 3 regions $S^{\rm conc}$, $S^{\rm dil}$and W (defined by solid lines). The $S^{\rm conc}$/W boundary defines a critical density-dependent reactivity, $Q = Q^*$. Region W is divided into two sub-regions by the $t_m^* = \tau$ line, above (below) which $t_m^* < \tau$ ($t_m^* > \tau$). The line $t_{\rm sat} = t_m^*$ is shown for the special case of constant $n_{\rm A}^\infty/n_{\rm B}^\infty$ (the convention is $n_{\rm A}^\infty \le n_{\rm B}^\infty$).

dense which determines the crossover time t_l. Later, we will return to eq. (2) with explicit expressions for $x(t)$.

Certain assumptions have been made in deriving eq. (2). It was implicit that $t_2^* < t_l < \tau$ since for $t > \tau$ chain center-of-gravity Fickian diffusion takes over and $x(t) \sim t^{1/2}$, *i.e.* $z = 2$ and $\mathcal{N}_{\rm coll}$ no longer increases with time; hence our previous arguments are invalid unless both t_2^* and t_l occur before τ. Our arguments also assumed that $t_2^* < t_l$; were this not true, then an A group could have encountered many B's and yet remain unreacted. These constraints limit

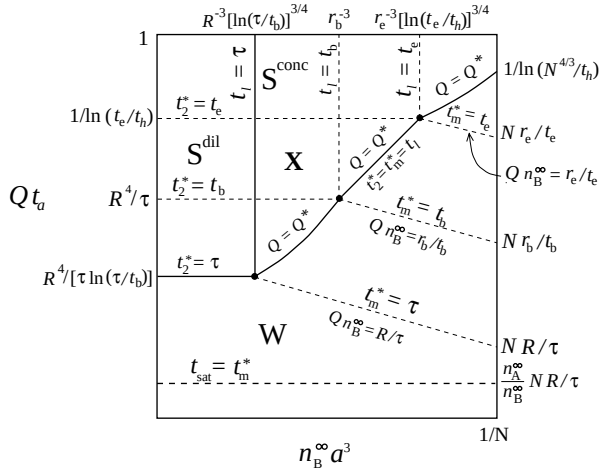

Fig. 3. – As fig. 2, but for entangled melts. Regions $S^{\rm conc}$, $S^{\rm dil}$and W now develop fine structure. In a given sub-region, relevant timescales occur within a given reptation diffusion regime thus defining a unique sequence of kinetic regimes.

the validity of eq. (2) to sufficiently high Q and $n_{\rm B}^{\infty}$ only. In the Q-$n_{\rm B}^{\infty}$ plane, these conditions are satisfied in the region marked $S^{\rm conc}$ (for strongly reactive, concentrated) in figs. 2 and 3.

Let us see first how the kinetics of eq. (2) are modified when Q and $n_{\rm B}^{\infty}$ have values such that $t_2^* > t_l$. Consider an A group initially within $x(t)$ of the interface. By time t it collides with the interface of order $(t/t_a)(h/x(t))$ times. Now since $t_2^* > t_l$, its reaction probability by t_l must be small; this means each such group collides with *many* B's before it reacts. Now each encounter with the interface produces reaction with probability $\approx n_{\rm B}^{\infty} a^3 Q t_a$. The net reaction probability $\lambda n_{\rm B}^{\infty} t/x(t) \sim t^{1-1/z}$ is thus increasing with time and becomes of order unity at t_m^*, where $x(t_m^*)/t_m^* = \lambda n_{\rm B}^{\infty}$. It follows that for $t > t_m^*$, all A groups within diffusive range of the interface will have reacted and a crossover occurs to 1st-order DC kinetics:

$$\mathcal{R}_t \;\approx\; \lambda\, t\, n_{\rm A}^{\infty} n_{\rm B}^{\infty} \;\xrightarrow{t_m^*}\; x(t)\, n_{\rm A}^{\infty} \quad (t_2^* > t_l \text{ or } t_2^* > \tau, \;\; \text{W})\,. \tag{3}$$

Notice the absence of 2nd-order DC kinetics. In fact, one can show eq. (3) is also valid if $t_2^* > \tau$. This is because reaction probability for a single pair always stops increasing after τ. In the Q-$n_{\rm B}^{\infty}$ plane of figs. 2 and 3, the conditions under which eq. (3) is valid correspond to region W, for "weakly reactive" (small Q).

The remaining region of the Q-$n_{\rm B}^{\infty}$ plane is that labeled $S^{\rm dil}$ ("strongly reactive, dilute") in figs. 2 and 3, corresponding to $t_2^* < \tau < t_l$. In this region all arguments leading to eq. (2) are still valid for $t < \tau$. But for $t > \tau$, $z = 2$ and reaction is no longer guaranteed when 2 groups are within diffusive range. Thus the hole in the 2-body correlation function stops growing and the 2nd-order DC kinetics cease. However, since $t_2^* < \tau$, reaction is certain when two coils overlap at the interface. Since by τ there is no density depletion at the interface, thus for $t > \tau$, the reaction rate is proportional to the equilibrium number of overlapping coils per unit area at the interface: $\mathcal{R}_t \approx (R^4/\tau) t\, n_{\rm A}^{\infty} n_{\rm B}^{\infty}$, where R is the polymer coil radius. Repeating the argument leading to the calculation of t_m^*, but replacing a and h by R and Q by $1/\tau$ leads to the conclusion that the reaction rate becomes limited by delivery of A species to the interface at a timescale $t_{m,R}^* = \tau (R^3 n_{\rm B}^{\infty})^{-2}$. In summary

$$\mathcal{R}_t \approx \lambda t n_{\rm A}^{\infty} n_{\rm B}^{\infty} \xrightarrow{t_2^*} x^4(t) n_{\rm A}^{\infty} n_{\rm B}^{\infty} \xrightarrow{\tau} (R^4/\tau) t n_{\rm A}^{\infty} n_{\rm B}^{\infty} \xrightarrow{t_{m,R}^*} x(t) n_{\rm A}^{\infty} \quad (t_2^* < \tau < t_l, S^{\rm dil})\,. \tag{4}$$

This completes the derivation of our general results, eqs. (2), (3) and (4). Let us now apply these to unentangled and entangled melts, respectively.

1) *Unentangled chains.* For shorter chain lengths N, Rouse dynamics apply [14], $x(t) \sim t^{1/4}$ for $t < \tau \approx N^2 t_a$. Ordinary Fickian diffusion, $x(t) \sim t^{1/2}$, onsets for $t > \tau$. Following the steps described above, the phase diagram of fig. 2 is constructed. Explicit formulae for timescales are obtained after inserting the appropriate $x(t)$ forms. The only complication is that the short time $z = 4$ regime is marginal ($\mathcal{N}_{\rm coll}$ increases only logarithmically with time). This leads to logarithmic corrections during the 2nd-order $x^4(t)$ DC kinetics:

$$\mathcal{R}_t \approx a^4 t/[t_a \ln(t/t_h)] n_{\rm A}^{\infty} n_{\rm B}^{\infty} \quad (\text{2nd order DC})\,, \tag{5}$$

where t_h is the diffusion time corresponding to h. Similarly, the $(R^4/\tau) t\, n_{\rm A}^{\infty} n_{\rm B}^{\infty}$ regime is modified to $\mathcal{R}_t \approx R^4 t/[\tau \ln(\tau/t_h)] n_{\rm A}^{\infty} n_{\rm B}^{\infty}$. These logarithmic corrections also modify the timescales t_2^*, t_l and $t_{m,R}^*$. From the results presented here, they are easily determined by demanding continuity of reaction rates.

As an example, consider a point in fig. 2 belonging to region $S^{\rm conc}$. The kinetic sequence is

$$\mathcal{R}_t \;\sim\; t\, n_{\rm A}^{\infty} n_{\rm B}^{\infty} \;\xrightarrow{t_2^*}\; (t/\ln t)\, n_{\rm A}^{\infty} n_{\rm B}^{\infty} \;\xrightarrow{t_l}\; t^{1/4} n_{\rm A}^{\infty} \xrightarrow{\tau}\; t^{1/2} n_{\rm A}^{\infty}\,. \tag{6}$$

2) *Entangled chains.* For N above the threshold N_e, entanglements onset. According to the "tube" or "reptation" model [14] Rouse dynamics apply for $t < t_{\rm e} \equiv N_e^2 t_a$ until $x(t)$

reaches the tube diameter $r_e \equiv N_e^{1/2}a$. The "breathing modes" $t^{1/8}$ regime follows, lasting until $t_b \equiv N^2 t_a$, while $x(t) \sim t^{1/4}$ for $t_b < t < \tau$, where $\tau \equiv (N^3/N_e)t_a$. Diffusion is Fickian for $t > \tau$.

Similarly to the unentangled case one constructs the phase diagram of fig. 3. The 3 basic regions $S^{\rm conc}$, $S^{\rm dil}$ and W now develop fine structure since each characteristic timescale may belong to different $x(t)$ regimes. (For example, for point X of fig. 3 one has $t_e < t_2^* < t_b$, and $t_b < t_l < \tau$.) Again, logarithmic corrections to the 2nd-order DC kinetics arise during the two short-time $t^{1/4}$ regimes, with $\mathcal{R}_t \approx a^4\ t/[t_a \ln(t/t_h)]n_A^\infty n_B^\infty$ during the first, and $\mathcal{R}_t \approx r_b^4\, t/[t_b \ln(t/t_b)]n_A^\infty n_B^\infty$ during the second (where $r_b \equiv N^{1/4}N_e^{1/2}a$).

As an example consider point X marked in fig. 3, belonging to the $S^{\rm conc}$ regime. Then eq. (2) implies:

$$\mathcal{R}_t \sim t\, n_A^\infty n_B^\infty \xrightarrow{t_2^*} t^{1/2} n_A^\infty n_B^\infty \xrightarrow{t_b} (t/\ln t)\, n_A^\infty n_B^\infty \xrightarrow{t_l} t^{1/4} n_A^\infty \xrightarrow{\tau} t^{1/2} n_A^\infty\,. \qquad (7)$$

Finally, let us consider effects of interfacial saturation by products. When $\mathcal{R}_t$ reaches the value $\mathcal{R}_{\rm crit} \equiv N^{-1/2}a^{-2}$, the diblocks start to feel one another laterally and therefore begin to stretch [5, 15]. Now during the very late stages, when $\mathcal{R}_t \gg \mathcal{R}_{\rm crit}$, incoming chains must overcome a very large free energetic barrier in order to react with the surface. It was shown in ref. [5] that this leads to a reaction rate decreasing exponentially with surface coverage, $\dot{\mathcal{R}}_t \sim e^{-9(\mathcal{R}_t/\mathcal{R}_{\rm crit})^2}$, which in turn implies that $\mathcal{R}_t$ increases logarithmically slowly in time, as demonstrated in ref. [7]. (For coverages greater than but of order $\mathcal{R}_{\rm crit}$, one expects $\dot{\mathcal{R}}_t \sim f(\mathcal{R}_t/\mathcal{R}_{\rm crit})$, where $f(u \gg 1) = e^{-9u^2}$. The detailed form of the crossover function f describes this intermediate regime. f is in principle available from eq. (1).)

Thus, for very large N, in effect reactions cease at coverages large compared to $\mathcal{R}_{\rm crit}$ (here we neglect destabilization effects which may increase interfacial area). Equating $\mathcal{R}_t$ to $\mathcal{R}_{\rm crit}$, we thus find that for all points well above a certain line (labeled $t_m^* = t_{\rm sat}$) in figs. 2 and 3, saturation occurs during the final 1st-order DC kinetics regime at a time $t_{\rm sat} = \tau/(N n_A^\infty a^3)^2$. Below that line, $t_{\rm sat} = 1/(Q n_A^\infty n_B^\infty h a^4 R)$ is smaller than t_m^* and saturation occurs before the crossover to the 1st-order DC regime.

We conclude with a brief discussion of our main findings. Since ordinary bimolecular rate constants correspond to $Qt_a \lesssim 10^{-6}$, experimental systems typically lie below the $t_{\rm sat} = t_m^*$ line of figs. 2 and 3. Then, apparently consistent with experiment [16], linear 2nd-order kinetics, $\mathcal{R}_t \sim t$, apply until surface crowding by products at $t_{\rm sat}$. As a specific example, if all chains were functionalized, $N = 300$ and $Qt_a \approx 10^{-6}$, then $t_{\rm sat}$ would be of order seconds. Typically groups are even less reactive and $t_{\rm sat}$ much longer. Note that if $n_A^\infty \ll n_B^\infty$ then even for small Qt_a a transition occurs to 1st-order DC kinetics. However, even in this case these kinetics may not be observable since t_m^* is likely to exceed reactive blending experimental timescales (of order minutes). We conclude that typical reactive blending experiments involving end-functionalized polymers are not in the DC regime. This would seem to be consistent with recent experiment [17].

Of considerable potential interest are experiments involving highly reactive radical species or strongly physically associating polymers, for which $Qt_a \approx 1$. For these, a range of 2nd- and 1st-order DC regimes are predicted. Measuring these various kinetic regimes with laser-induced radicals thus offers an interesting probe of fundamentals of interfacial polymer dynamics.

***

This work was supported by the National Science Foundation, grant no. DMR-9403566. We thank U. SAWHNEY for stimulating discussions.

REFERENCES

[1] Sperling L. H., *Polymeric Multicomponent Materials: an Introduction* (Wiley, New York) 1997.
[2] Beck Tan N. C., Tai S.-K. and Briber R. M., *Polymer*, **37** (1996) 3509.
[3] Kramer E., Norton L. J., Dai C.-A., Sha Y. and Hui C.-Y., *Faraday Discuss.*, **98** (1994) 31.
[4] Gersappe D., Irvine D., Balazs A. C., Liu Y., Sokolov J., Rafailovich M., Schwarz S. and Peiffer D. G., *Science*, **265** (1994) 1072.
[5] O'Shaughnessy B. and Sawhney U., *Phys. Rev. Lett.*, **76** (1996) 3444; *Macromolecules*, **29** (1996) 7230.
[6] Fredrickson G. H., *Phys. Rev. Lett.*, **76** (1996) 3440.
[7] Fredrickson G. H. and Milner S. T., *Macromolecules*, **29** (1996) 7386.
[8] Muller M., *Macromolecules*, **30** (1997) 6353.
[9] Guégan P., Macosko C. W., Ishizone T., Hirao A. and Nakahama S., *Macromolecules*, **27** (1994) 4993.
[10] Kotomin E. and Kuzovkov V., *Modern Aspects of Diffusion-Controlled Reactions; Cooperative Phenomena in Bimolecular Processes*, edited by R. G. Compton and G. Hancock (Elsevier, Amsterdam) 1996.
[11] O'Shaughnessy B. and Vavylonis D., http://xxx.lanl.gov/abs/cond-mat/9807110, submitted to *Eur. Phys. J. B*.
[12] O'Shaughnessy B., *Phys. Rev. Lett.*, **71** (1993) 3331; *Macromolecules*, **27** (1994) 3875.
[13] Friedman B. and O'Shaughnessy B., *Europhys. Lett.*, **23** (1993) 667; *Macromolecules*, **26** (1993) 5726.
[14] Doi M. and Edwards S. F., *The Theory of Polymer Dynamics* (Clarendon Press, Oxford) 1986.
[15] Semenov A. N., *Sov. Phys. JETP*, **61** (1985) 733.
[16] Scott C. and Macosko C., *J. Polym. Sci. B*, **32** (1994) 205.
[17] Orr C. A., Adedeji A., Hirao A., Bates F. S. and Macosko C. W., *Macromolecules*, **30** (1997) 1243.